Received: 13 December 2020 | Revised: 23 January 2021 | Accepted: 25 January 2021

DOI: 10.1002/rcm.9062

RESEARCH ARTICLE

Rapid Communications in Mass Spectrometry WILEY

Study of the isomeric Maillard degradants, glycosylamine and Amadori rearrangement products, and their differentiation via MS^2 fingerprinting from collision-induced decomposition of protonated ions

Shaolan Wang[1,2] | Jinsheng Lin[1] | Dan Li[1] | Tianpei Huang[1] | Wenquan Zhu[1] | Wenbin Chen[1] | Min Li[1,3] | Weiyang Shen[2]

[1]Center of Excellence for Modern Analytical Technologies (CEMAT), Zhejiang Huahai Pharmaceutical Co. Ltd., Xunqiao, Linhai, Zhejiang, 317204, China

[2]Department of Pharmaceutical Analysis, China Pharmaceutical University, Nanjing, 210009, China

[3]Huahai US, Inc., 700 Atrium Drive, Somerset, NJ, 08873, USA

Correspondence
M. Li, Center of Excellence for Modern Analytical Technologies (CEMAT), Zhejiang Huahai Pharmaceutical Co. Ltd, Xunqiao, Linhai, Zhejiang 317204, China.
Email: minli88@yahoo.com

W.-Y. Shen, Department of Pharmaceutical Analysis, China Pharmaceutical University, Nanjing 210009, China.
Email: shenweiyang@cpu.edu.cn

Rationale: The focus of this work was to study glycosylamine and Amadori rearrangement products (ARPs), the two major degradants in the Maillard reactions of pharmaceutical interest, and utilize their MS^2 fingerprints by liquid chromatography/high-resolution tandem mass spectrometry ($LC/HRMS^2$) to quickly distinguish the two isomeric degradants. These two types of degradants are frequently encountered in the compatibility and stability studies of drug products containing primary or secondary amine active pharmaceutical ingredients (APIs), which are formulated with excipients consisting of reducing sugar functionalities.

Methods: Vortioxetine was employed as the primary model compound to react with lactose to obtain the glycosylamine and ARP degradants of the Maillard reaction, and their MS^2 spectra (MS^2 fingerprints) were obtained by LC/MS^2. Subsequently, the two degradants were isolated via preparative HPLC and their structures were confirmed by one- and two-dimensional (1D and 2D) nuclear magnetic resonance (NMR) determination.

Results: The MS^2 fingerprints of the two degradants display significantly different profiles, despite the fact that many common fragments are observed. Specifically, protonated glycosylamine shows a prominent characteristic fragment of $[M_{vort} + C_2H_3O]^+$ at *m/z* 341 (M_{vort} is the vortioxetine core), while protonated ARP shows a prominent characteristic fragment of $[M_{vort} + CH]^+$ at *m/z* 311. Further study of the Maillard reactions between several other structurally diverse primary/secondary amines and lactose produced similar patterns.

Conclusions: The study suggests that the characteristic MS^2 fragment peaks and their ratios may be used to differentiate the glycosylamine and ARP degradants, the two isomeric degradants of the Maillard reaction, which are commonly encountered in finished dosage forms of pharmaceutical products containing primary and secondary amine APIs.

1 | INTRODUCTION

Drug degradation products, or drug degradants, are inevitably formed in drug products which are formally examined in various drug stability studies, such as long-term[1] and accelerated stability studies[2] under the ICH stability conditions. The rapid structural elucidation of drug degradants is critical to the quality and safety of a drug product. For formulated drug products, drug degradation can originate from the interaction (or incompatibility) between the active pharmaceutical ingredient (API) and excipients. The Maillard reaction is one of the major reasons for the chemical incompatibility encountered during pharmaceutical development.[3–5] Over 100 years ago, Louis Maillard reported that carbonyl compounds may react with amino acids and proteins to produce complex mixtures of brown pigments; this phenomenon has become known as the Maillard reaction.[6] Pharmaceutical formulations containing primary and secondary amine APIs as well as excipients of reducing sugars are prone to this degradation chemistry, in which condensation between the amines and aldehyde functional groups takes place as the initial step of the Maillard reaction, resulting in the formation of Schiff bases, which cyclize to become glycosylamines, under pharmaceutically relevant conditions. The glycosylamines may not be stable enough and, quite often, they can undergo the Amadori rearrangement to form 1-deoxy-1-amino-2-ketoses, also known as the Amadori rearrangement products (ARPs).[7] The Maillard reaction is a very complex process; only the early-stage degradants, namely the initial glycoylsamine and possibly the ARP degradants, are usually relevant in drug degradation chemistry.[8] While the formation of the initial Schiff base/glycosylamine may be reversible, that of the ARPs is irreversible. In addition, an ARP is also a key intermediate for a number of subsequent degradants containing aldehyde and α-diketo functional groups. Thus, it is important to distinguish the glycosylamine and ARP degradants.

Nevertheless, the glycosylamine and ARP degradants are isomeric toward each other; hence, they are not distinguishable based on their molecular weights or formulae. In our laboratories, we have employed a strategy that combines liquid chromatography/photo-diode array UV/multi-stage mass spectrometry (LC/PDA-UV/MS^n) with mechanism-based stress studies to rapidly elucidate the structures of unknown degradants with a very high confidence level.[9–17] The most critical and reliable component of this strategy is the MS^n molecular fingerprints, which can be used to differentiate structurally similar diastereomers, through the often subtle but distinguishable differences between their MS^n fingerprints.[18] Therefore, in the current study, we envisaged that the MS^n fingerprints of the two isomeric Maillard degradants would be different and, as such, certain fragments in the two isomers might be utilized as characteristic markers to differentiate them. Such an approach would be much more efficient than alternative analytical techniques such as nuclear magnetic resonance (NMR) spectroscopy. Thus, we decided to use vortioxetine, a drug for treating major depression,[19] as the primary model compound containing a secondary amine moiety to react with lactose, one of the most utilized reducing sugars in pharmaceutical formulations,[20] to generate the corresponding glycosylamine and ARP degradants (1 and 2; Scheme 1) for analysis by high-resolution LC/MS^n molecular fingerprinting.

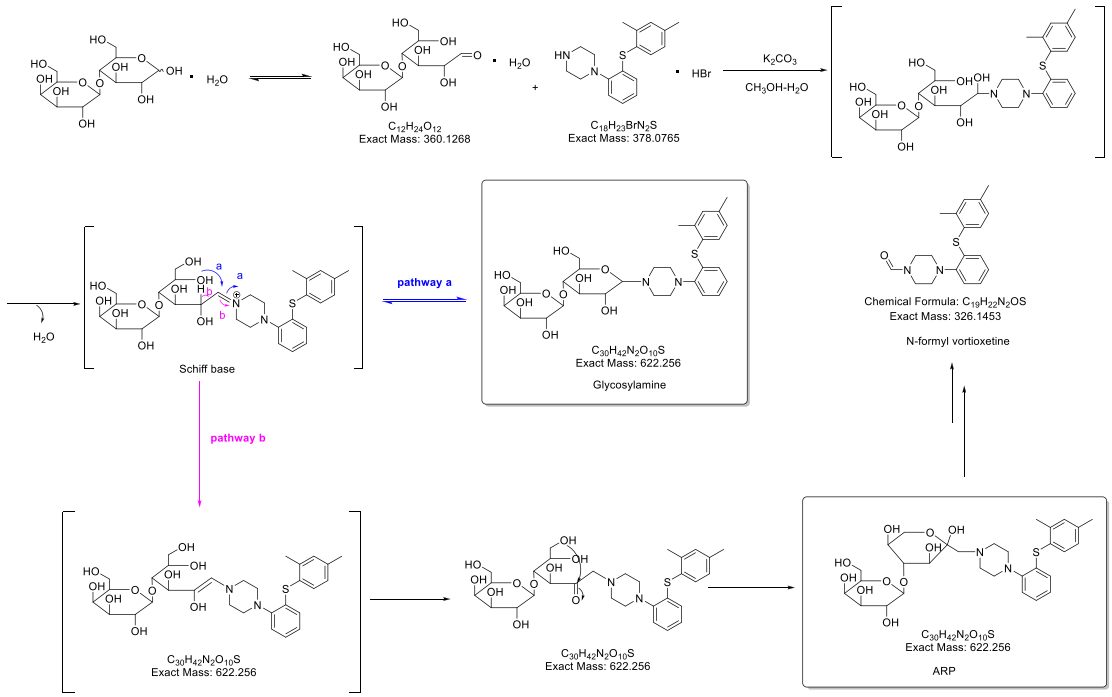

SCHEME 1 A plausible mechanism for the reaction between vortioxetine and lactose; pathway b is the Amadori rearrangement

In the subsequent study, the corresponding Maillard reaction degradants obtained from reactions of vortioxetine with other reducing sugars (degradants 3 through 6), as well as several other structurally diverse primary/secondary amines with lactose, glucose, and galactose (degradants 7 through 16), were subjected to the same high-resolution LC/MS^n analysis.

Here we will demonstrate that two characteristic fragments obtained from the MS^2 fragmentation and their ratios may be used to rapidly differentiate the glycosylamine and ARP degradants of the Maillard reaction. During the final stage of preparing this manuscript for publication, we have become aware of the work just published by Xing et al,[21,22] in which they reported that MS/MS fragmentation patterns can be used to discriminate between glucose-derived Schiff bases, Amadori, and Heyns compounds with several amino acids. Their work as well as ours indicates that this methodology can be generally applicable for differentiating the early-stage isomeric Maillard products from amino compounds of vastly different structures with reducing sugars.

2 | EXPERIMENTAL

2.1 | Chemicals and reagents

Vortioxetine was manufactured by Zhejiang Huahai Pharmaceutical Co., Ltd (Linhai, Zhejiang, China). Acetonitrile and ethanol were purchased from Sigma-Aldrich Corp. (St Louis, MO, USA). Formic acid, dimethyl sulfoxide (DMSO), dimethylformamide (DMF), lactose, glucose, galactose, α-phenylethylamine, 1-phenylpiperazine and benzylamine were procured from Shanghai Aladdin Biochemical Technology Co., Ltd (Shanghai, China). Ammonium acetate and sodium carbonate were purchased from Xilong Chemical Co., Ltd (Guangdong, China).

2.2 | HPLC conditions

2.2.1 | Method I

A Dionex Ultimate 3000 HPLC system (Thermo Scientific, Waltham, MA, USA) equipped with a YMC PACK ODS-AQ column (250 mm × 4.6 mm, 5 μm) and a PDA-UV detector was used to analyze the Maillard reaction results. The mobile phase system consisted of A (water with 600 mg/L ammonium acetate) and B (acetonitrile), with the gradient varied according to the following program: 0 min (40% B), 10 min (40% B), 25 min (90% B), 30 min (90% B), 30.1 min (40% B), and 33 min (40% B). The analyses were performed at a flow rate of 1.0 mL/min and a column temperature of 40°C. UV spectra were collected between 190 and 400 nm by the PDA-UV detector and, for UV chromatograms, a wavelength of 250 nm was used. This method was used in the experiments involving the Maillard reaction with vortioxetine.

2.2.2 | Method II

The mobile phase gradient was varied according to the following program: 0 min (40% B), 1 min (40% B), 10 min (90% B), 12 min (90% B), 12.1 min (40% B) and 15 min (40% B). The other parameters were the same as for method I. This method was used in the experiments involving the Maillard reaction with other primary and secondary amines. Due to the fact that the elution times of the relevant components in the Maillard reaction were significantly shorter than those in the Maillard reaction with vortioxetine, the run time of this method is approximately half of that in method I.

2.3 | LC/PDA-UV/MS^n (n = 1, 2) analysis

A 1260 series HPLC instrument (Agilent Technologies, Santa Clara, CA, USA) interfaced to a quadrupole time-of-flight (Q-TOF) mass spectrometer (6545 series, Agilent Technologies) was used for comprehensive LC/PDA-UV/MS^n (n = 1, 2) analyses of samples. UV spectra were collected from 190 nm to 400 nm by the PDA detector. The Q-TOF mass spectrometer was operated in positive electrospray ionization (ESI) mode with the following source parameters: fragmentor voltage 70 V, gas flow 6 L/min, nebulizer pressure 60 psi, source temperature 320°C, sheath gas temperature 350°C, sheath gas flow 12 L/min, and capillary voltage 3.5 kV. Nitrogen was used as the gas for all purposes including collision-induced decomposition (CID). The mass acquisition range was *m/z* 100–1700 and, for the MS^2 analyses, the collision energy was set at 10, 20, and 30 eV, respectively. The chromatographic conditions of the LC/MS method were the same as those of method I.

Some of the LC/PDA-UV/MS^n experiments were also conducted on an IT-TOF mass spectrometer (Shimadzu, Kyoto, Japan). The IT-TOF mass spectrometer was operated in positive ESI mode with the following parameters: nebulizing gas flow 1.5 L/min, drying gas pressure 107 kPa, CDL temperature 200°C, heating block temperature 200°C, detector voltage 1.6 kV, ion accumulation time 50 ms, and interface voltage 4.5 kV. Nitrogen was used as the gas for all purposes except CID, for which argon was used. The mass acquisition range was *m/z* 50–1000 and, for the MS^2 analyses, the collision energy was set at 50%. The chromatographic conditions of the LC/MS method were the same as those for method I.

2.4 | Maillard reaction between vortioxetine and lactose

A mixture of vortioxetine (5 mg), lactose monohydrate (47.55 mg), and potassium carbonate (3.6 mg) in 1.2 mL water/acetonitrile (50:50, v/v) was shaken at 60°C for 24 h. Aliquots of the reaction solution were analyzed by HPLC and LC/MS^n (n = 1, 2) as described in sections 2.2.1 and 2.3, respectively.

2.5 | Preparation and isolation of glycosylamine 1 produced by the Maillard reaction between vortioxetine and lactose

A relatively large quantity of the degradation product of vortioxetine and lactose was needed for further investigation. Hence, a mixture of vortioxetine (1 g), lactose monohydrate (9.51 g), and potassium carbonate (0.72 g) in 120 mL water/acetonitrile (50:50, v/v) was allowed to stir at 60°C for 24 h. After reaction, the solvent was removed by rotary evaporator. Then 100 mL ethanol was added and the solution was allowed to stir at room temperature for 30 min. The insoluble potassium carbonate was filtered and the filtrate was concentrated to 10 mL. The mixture was loaded onto a LC-8A series preparative HPLC instrument (Shimadzu) for isolation of the product. The preparative HPLC instrument was equipped with a YMC PACK ODS-AQ column (250 mm × 20 mm, 5 μm) and a UV detector. The mobile phase system consisted of A (water with 0.6 g/L ammonium acetate) and B (acetonitrile), with the gradient varied according to the following program: 0 min (40% B), 10 min (40% B), 25 min (90% B), 30 min (90% B), 30.1 min (40% B) and 33 min (40% B). The analyses were performed at a flow rate of 15 mL/min and the fractions at ~15–16 min were collected, combined, and then lyophilized to afford 220 mg of product (22% yield).

2.6 | Selection of the optimal conditions for converting glycosylamine 1 into ARP 2

Six 1.5 mL HPLC vials were selected and labeled as vials 1, 2, 3, 4, 5 and 6. Then 1 mg of the isolated glycosylamine 1 solid sample was added to each of the six vials. To vials 2, 3, 4, 5 and 6, 1 mL each of the following solvents was added into each vial, respectively: water, methanol, acetonitrile, DMF, and DMSO. The glycosylamine in vial 1 remained in the solid state. All the vials were capped and then

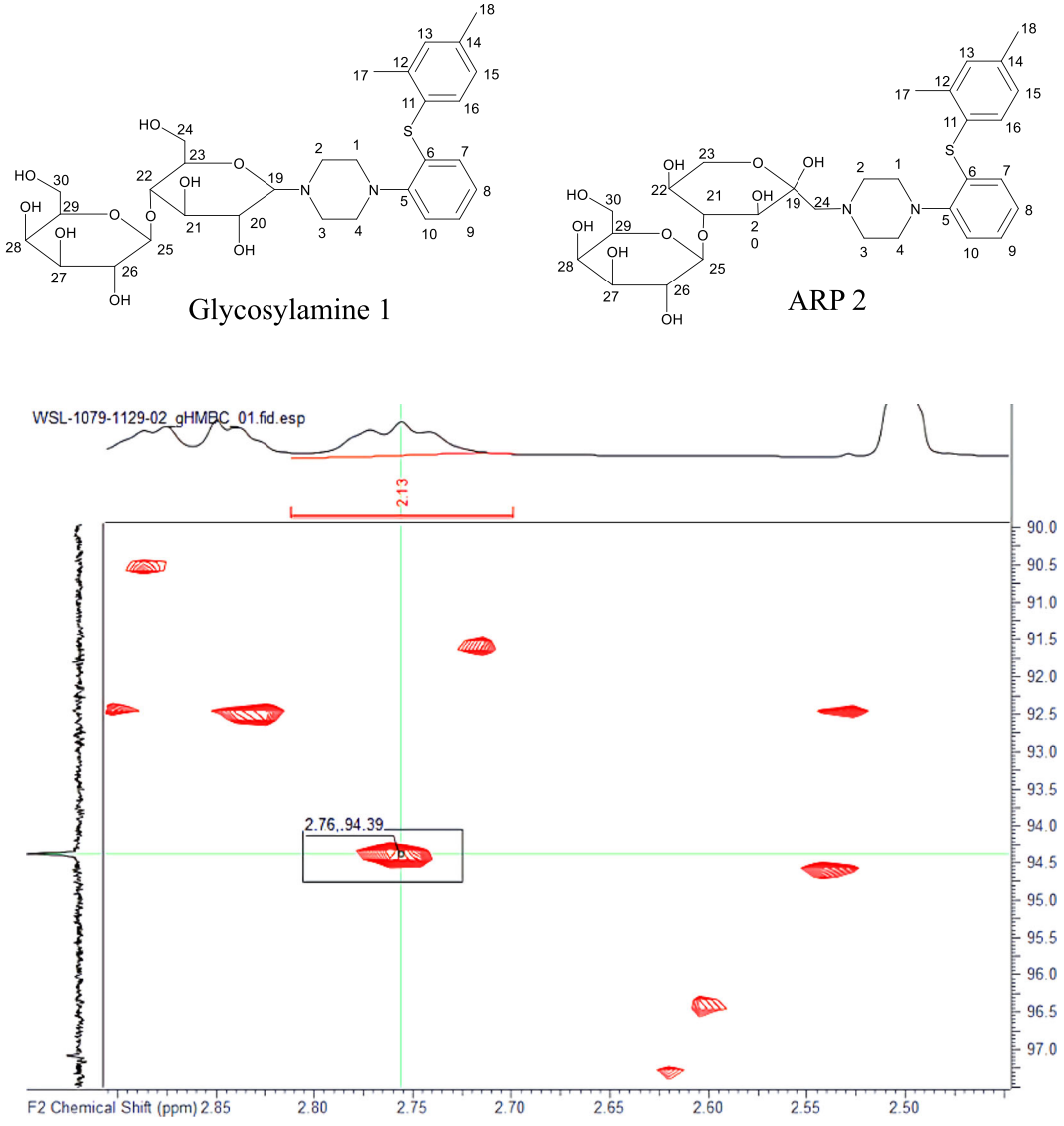

FIGURE 1 The key gHMBC correlations of glycosylamine 1 formed between vortioxetine and lactose

heated at 80°C for 24 h with vibration. Samples of the reaction solid (vial 1) and solutions (vials 2 to 6) were analyzed by HPLC and LC/MS^n (n = 1, 2) as described in sections 2.2.1 and 2.3, respectively; the solid sample in vial 1 was dissolved in methanol (1 mg/mL) prior to injection, while all the solution samples were diluted with methanol (1 mg/mL) and then injected (5 μL). The results show that the highest yield of ARP 2 was achieved at ~27% in vial 1.

2.7 | Isolation of ARP 2

A relatively large quantity of ARP 2 was needed for NMR structural confirmation. Based on the results of section 2.6, a 20 mL headspace GC vial was selected as the reaction vessel in which 40 mg of the isolated glycosylamine 1 was placed, which was heated at 80°C for 24 h with shaking. After that, 10 mL methanol was added to dissolve the solid. The mixture was then loaded onto the preparative HPLC instrument (LC-8A series, Shimadzu) for isolation of the product. The preparative HPLC instrument was equipped with a YMC PACK ODS-AQ column (250 mm × 25 mm, 5 μm) and a UV detector. The mobile phase system consisted of A (water with 0.6 g/L ammonium acetate) and B (acetonitrile), with the gradient varied according to the following program: 0 min (40% B), 10 min (40% B), 25 min (90% B), 30 min (90% B), 30.1 min (40% B) and 33 min (40% B). The purification was performed at a flow rate of 15 mL/min and the fractions at ~17–18 min were collected. The fractions collected from different runs were combined, and then lyophilized to afford ~10 mg of the product (2; 25% yield).

2.8 | 1D and 2D NMR determination of glycosylamine 1 and ARP 2

Approximately 10 mg of glycosylamine 1 and 10 mg of ARP 2, prepared and isolated as described in sections 2.5 and 2.7, were dissolved in 1 mL of $CDCl_3$, respectively. ^{1}H-, ^{13}C-NMR and 2D NMR

TABLE 1 ^{1}H-NMR and ^{13}C-NMR data of glycosylamine 1 formed between vortioxetine and lactose

C δ (ppm)	C type	C number	H δ (ppm)	Peak	H number	Position
20.6	CH_3	1	2.23	s	3	17
21.2	CH_3	1	2.32	s	3	18
47.4	CH_2	2	2.76/3.03	t	4	2, 3
52.0	CH_2	2	2.97	t	4	1, 4
60.8	CH_2	1	3.51	d	2	24
61.2	CH_2	1	3.59/3.75	dd	2	30
68.5	CH	1	3.62	m	1	27
69.4	CH	1	3.33	m	1	20
71.0	CH	1	3.32	m	1	26
73.7	CH	1	3.31	m	1	28
76.0	CH	1	3.44	m	1	22
76.4	CH	1	3.34	o	1	21
76.9	CH	1	3.23	d	1	23
81.4	CH	1	3.25	o	1	29
94.4	CH	1	3.83	d	1	19
104.3	CH	1	4.22	d	1	25
120.3	CH	1	7.10	o	1	10
124.6	CH	1	6.88	t	1	8
125.6	CH	1	6.33	d	1	7
126.1	CH	1	7.08	o	1	9
127.7	C	1	-	-	-	11
128.5	CH	1	7.10	o	1	15
132.1	CH	1	7.24	br s	1	13
134.0	C	1	-	-	-	6
136.5	CH	1	7.35	d	1	16
140.0	C	1	-	-	-	14
142.3	C	1	-	-	-	12
150.0	C	1	-	-	-	5

The numbering of the carbon skeleton in glycosylamine 1 is shown in Figure 1.
o, overlapping signals; br s, broad singlet signal.

spectra of the two compounds were acquired on a 400 MHz spectrometer (Agilent Technologies) at 25°C. ^{1}H and ^{13}C resonances were assigned and confirmed by the results from the following 2D NMR experiments: gCOSY, gHSQC, and gHMBC.

2.9 | Studies of the Maillard reactions of other model amino compounds with reducing sugars

To explore the general applicability of using the MS^2 molecular fingerprinting for differentiating glycosylamines and ARPs, the Maillard reactions of vortioxetine with other reducing sugars were also examined. Hence, vortioxetine (50 mg) was reacted with glucose (240 mg) and galactose (240 mg), respectively, in solutions of 6 mL water and 6 mL acetonitrile containing potassium carbonate (36 mg), resulting in reaction mixtures A and B.

On the other hand, the Maillard reactions of other primary and secondary amines with lactose or galactose were also explored. Hence, 10 μL α-phenylethylamine and 280 mg lactose were dissolved in 6 mL water and 6 mL acetonitrile, resulting in reaction mixture C. Likewise, benzylamine and 1-phenylpiperazine were mixed with lactose in solution in the same fashion, resulting in reaction mixtures D and E, respectively. Finally, benzylamine (10 μL) was reacted with glucose (165 mg) and galactose (165 mg), respectively, in solutions of 6 mL water and 6 mL acetonitrile, resulting in reaction mixtures F and G.

All the mixtures were heated at 80°C for 24 h with shaking. Aliquots of mixtures A and B were analyzed by HPLC and LC/MS^n (n = 1, 2) as described in sections 2.2.1 and 2.3, respectively. Aliquots of mixtures C through G were analyzed by LC/MS^n (n = 1, 2) as described in section 2.3.

3 | RESULTS AND DISCUSSION

Glycosylamine 1 and ARP 2 degradants generated from the Maillard reaction between vortioxetine and lactose are novel compounds that have not been reported previously; they have been fully characterized by LC/MS, ^{1}H- and ^{13}C-NMR in this study, which will be described in detail below.

3.1 | $LC/PDA\text{-}UV/MS^n$ analysis of glycosylamine 1

Vortioxetine was reacted with lactose in order to obtain the degradants of the Maillard reaction which was outlined in section 2.4. In the UV chromatogram, a peak at 15.600 min was observed in ~31% yield, the accurate *m/z* value of which was 623.2598 (refer to Figures S1 and S2, respectively, supporting information), consistent with the formula of the adduct formed between vortioxetine and lactose in protonated form, i.e., $[C_{30}H_{42}N_2O_{10}S + H^+]$, within an error of −5.6 ppm. This adduct was suspected to be glycosylamine 1 as it

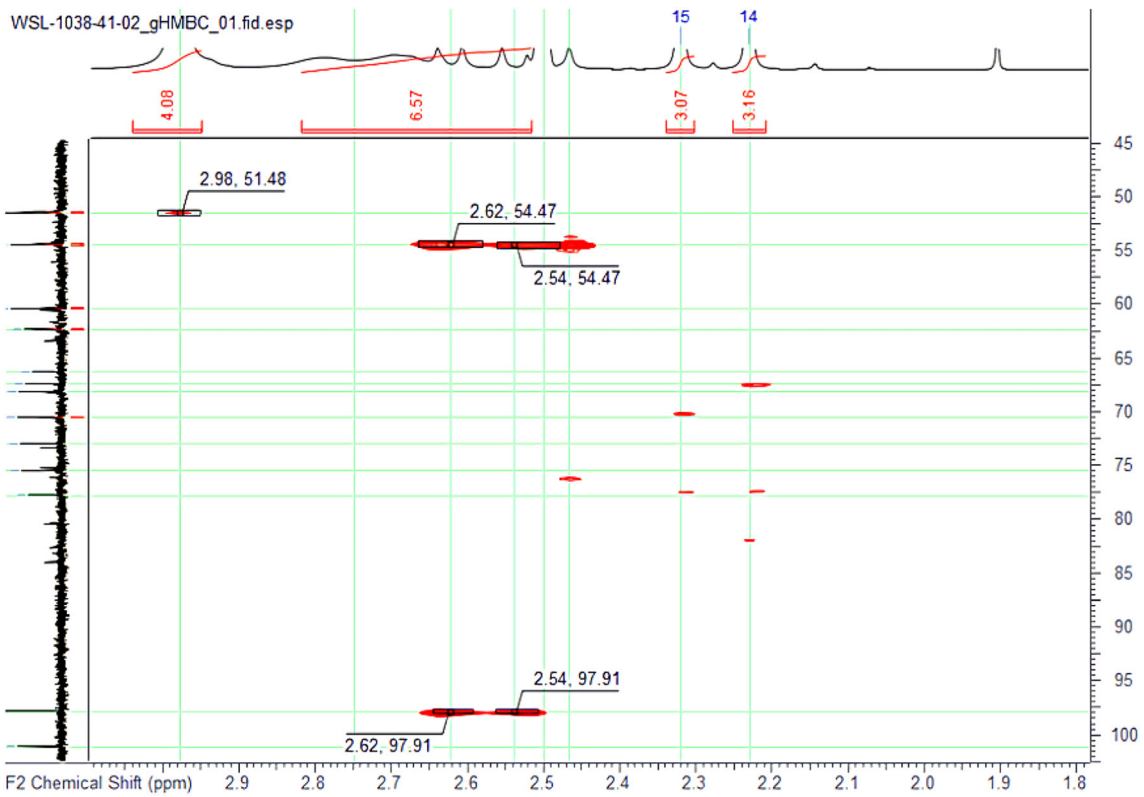

FIGURE 2 The key gHMBC correlations of ARP 2 formed between vortioxetine and lactose

was the first product formed in the Maillard reaction and, thus, it would usually be the main product observed in the early stage of the Maillard reaction.

3.2 | Structural characterization of glycosylamine 1 by 1D and 2D NMR

In order to confirm the structure of the degradant, approximately 10 mg of the isolated degradant was analyzed by 1D and 2D NMR. The ^{13}C-NMR spectrum showed that it has 30 carbon atoms. The ^{1}H-NMR and gHSQC spectra indicated that it contains two methyl groups, six methylene groups, seventeen methine groups, and five quaternary carbons, among which seven methine groups are in the aromatic region. These results match the structure of glycosylamine 1. More specifically, δH 2.76 (H-2,3) is related to δC 94.4 (C-19) in the gHMBC spectrum (Figure 1), further indicating that the degradant is glycosylamine 1 that was formed between the amino moiety of vortioxetine and the glucose moiety of lactose (Table 1).

3.3 | Conversion of glycosylamine 1 into ARP 2

In addition to ~31% glycosylamine 1, the experiment described in section 2.4 also produced a species that eluted at 17.863 min with a yield of 1.48%. Its protonated ion was at *m/z* 623.2622, matching the formula of $[C_{30}H_{42}N_2O_{10}S + H^+]$ within an error of −1.76 ppm, which is the same as the molecular formula of glycosylamine 1. It was suspected that the 17.863 min species is ARP 2. Nevertheless, its content was too low to be isolated for NMR analysis. According to the mechanism of the Maillard reaction, glycosylamine would isomerize to ARP. Hence, conversion of glycosylamine 1 into ARP 2 was tried under different conditions including heating glycosylamine 1 in various solvents as well as in the solid state.

The results showed that the yield of the suspected ARP 2 was ~3% in various solvents. This yield was still too low, which would

TABLE 2 ^{1}H-NMR and ^{13}C-NMR data of the Amadori rearrangement product (ARP 2) formed between vortioxetine and lactose

C δ (ppm)	C type	C number	H δ (ppm)	Peak	H number	Position
20.2	CH_3	1	2.23	s	3	17
20.8	CH_3	1	2.32	s	3	18
51.5	CH_2	2	2.98	m	4	1,4
54.5	CH_2	2	2.75	m	4	2,3
60.4	CH_2	1	3.51	o	2	23
62.4	CH_2	1	3.48, 3.81	d	2	30
62.4	CH_2	1	2.54, 2.62	d	2	24
66.3	CH	1	3.88	m	1	29
67.5	CH	1	3.66	m	1	26
68.2	CH	1	3.62	m	1	20
70.6	CH	1	3.39	o	1	22
73.0	CH	1	3.33	o	1	28
75.5	CH	1	3.38	o	1	21
77.8	CH	1	3.78	dd	1	27
97.9	C	1	-	-	-	19
101.2	CH	1	4.26	d	1	25
120.1	CH	1	7.13	d	1	10
124.3	CH	1	6.89	t	1	8
125.5	CH	1	6.35	d	1	7
125.8	CH	1	7.09	t	1	9
127.3	C	1	-	-	-	12
128.1	CH	1	7.08	d	1	15
131.7	CH	1	7.23	br s	1	13
133.4	C	1	-	-	-	6
135.9	CH	1	7.33	d	1	16
139.2	C	1	-	-	-	14
141.8	C	1	-	-	-	11
149.1	C	1	-	-	-	5

The numbering of the carbon skeleton in ARP 2 is shown in Figure 1.
o, overlapping signals; br s, broad singlet signal.

make the preparation and isolation of ARP 2 quite difficult. On the other hand, heating glycosylamine 1 in the solid state at 80°C for 24 h generated the suspected ARP (2; the 17.867 min peak) in ~25% of isolated yield. The *m/z* value of the protonated ion was 623.2606 (refer to Figures S3 and S4, respectively, supporting information), matching the formula of $[C_{30}H_{42}N_2O_{10}S + H^+]$ within an error of −4.3 ppm, which is consistent with the protonated ARP 2 and isomeric with the protonated glycosylamine 1.

3.4 | Structural characterization of ARP 2 by 1D and 2D NMR

In order to confirm that the degradant is ARP 2, approximately 10 mg of the isolated degradant was analyzed by 1D and 2D NMR. The ^{13}C-NMR spectrum showed 30 carbon atoms: two methyl groups, seven methylene groups, fifteen methine groups, and six quaternary carbons, among which seven methine groups are in the aromatic region. Its overall structure is quite similar to that of glycosylamine, except for the following differences: it has one more methylene group and quaternary carbon, but one less methine group. In its gHMBC spectrum (Figure 2), δH 2.54/2.62 (H-24), δC 54.5 (C-2, 3), and δC 97.9 (C-19) are related, indicating that the degradant at 17.867 min is indeed ARP 2 (Table 2). It needs to be pointed out that ARP 2 is in the cyclized form of pyranose.

3.5 | *N*-Formyl vortioxetine: Degradation product of ARP

In addition to ARP 2, the solid sample of glycosylamine also decomposed to give back vortioxetine in ~17.6% yield and a peak at 24.920 min in ~4% yield in the course of 80°C heating for 24 h. The protonated ion of the 24.920 min species showed an ion at *m/z* 327.1522, matching a formula of $[C_{19}H_{22}N_2OS + H^+]$. The latter formula has an extra CO group than that of vortioxetine, suggesting it is likely *N*-formyl vortioxetine, which was later confirmed via NMR analysis of the isolated impurity.[23] It has been reported that this type of *N*-formyl degradant can originate from the Maillard reaction.[24]

All the Maillard reaction pathways described above are summarized in Scheme 1.

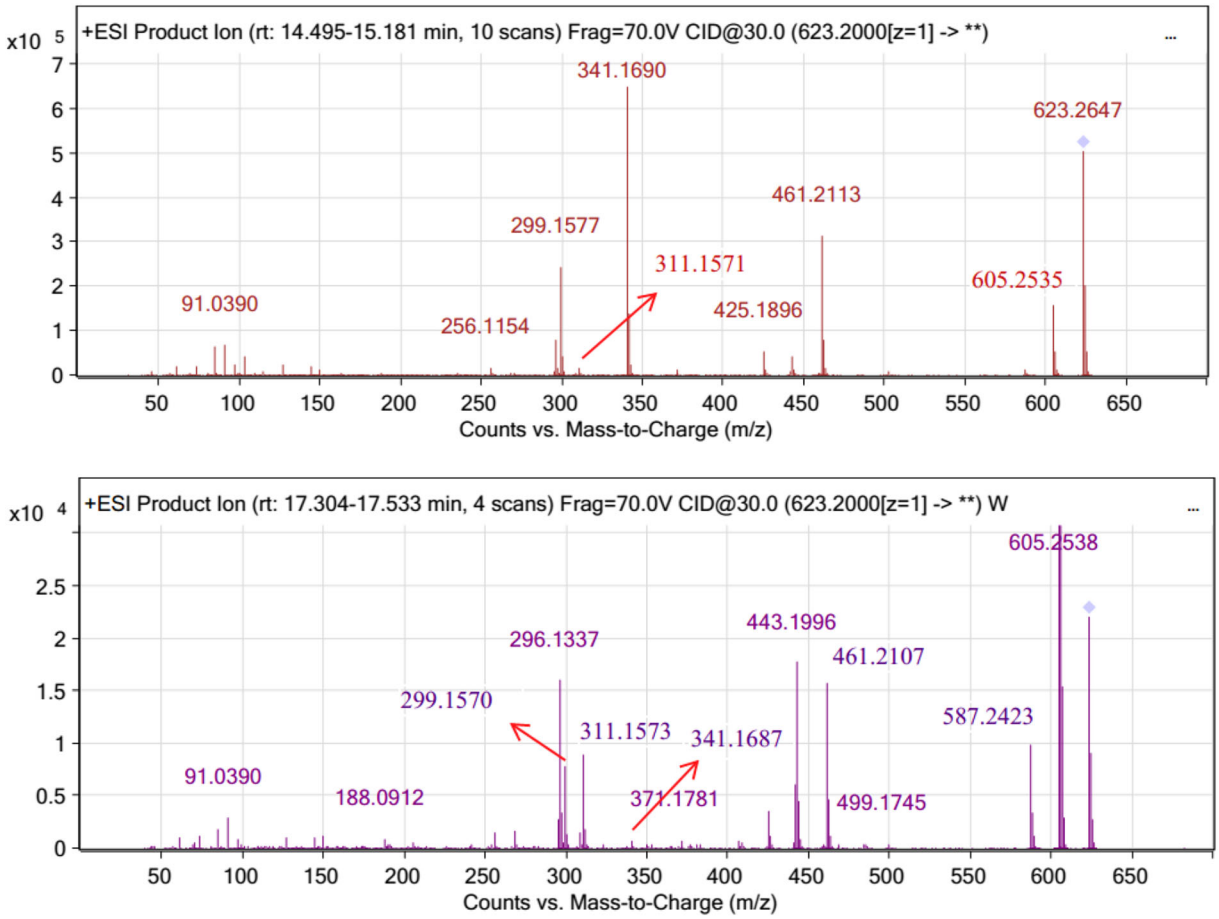

FIGURE 3 Top: CID-MS^2 of glycosylamine 1. The abundance of *m/z* 341 was much greater than the abundance of *m/z* 311 and the ratio of *m/z* 341 to *m/z* 311 was ~32. Bottom: CID-MS^2 of ARP 2. The abundance of *m/z* 311 was greater than the abundance of *m/z* 341 and the ratio of *m/z* 311 to *m/z* 341 was ~11

3.6 | Differentiation of glycosylamine 1 and ARP 2 via their MS^2 fingerprints obtained from high-resolution LC/MS^2

3.6.1 | CID-MS^2 fragmentation/fingerprinting of the precursor ions of glycosylamine 1 and ARP 2

It should be noted that glycosylamine 1 and ARP 2 are isomers and it would be very difficult to distinguish them by single-stage mass spectrometry unless the analysis was performed by an MS instrument equipped with ion mobility capability. The molecular structures of glycosylamine 1 and ARP 2 were established in the previous sections by 1D and 2D NMR. The main focus of this paper is to differentiate between these two isomers via their low-energy CID MS/MS analyses and the establishment of their unique fingerprinting.

Collision-induced decomposition MS^2 (CID-MS^2) of the protonated glycosylamine (1, Figure 3, top), obtained at a collision energy (CE) of 30 eV, exhibited several major product ions at *m/z* 605, 461, 341, and 299, among which the *m/z* 299 ion coincides with the protonated ion of vortioxetine. The most abundant fragment is *m/z* 341, which appears to stem from β-fission of the open-ring form (Schiff base) of glycosylamine (Pathway a, Scheme 2). Loss of formaldehyde from *m/z* 341 would produce the weak *m/z* 311 fragment. A plausible mechanism for the fragmentation pathways of glycosylamine 1 is proposed in Scheme 2.

The CID-MS^2 spectra of the protonated ARP (2, Figure 3, bottom), obtained at a CE of 30 eV, showed the following major product ions at *m/z* 605, 587, 498, 443, 311, and 296. The abundance of the *m/z* 605 ion is particularly high, which is 18 less than the *m/z* 623 ion, suggesting the presence of a hydroxyl group that is particularly easy to cleave from ARP 2. This observation appears to be consistent with the presence of a hydroxyl group at position-19 of ARP 2 (Pathway a, Scheme 3). The *m/z* 587 ion is formed from the double dehydration of the protonated ARP 2. The *m/z* 443 ion seems to result from the cleavage of *m/z* 461 by loss of H_2O. The *m/z* 299 fragment, which should correspond to protonated ARP 2, is also present. A plausible mechanism for the fragmentation pathways of ARP 2 is proposed in Scheme 3.

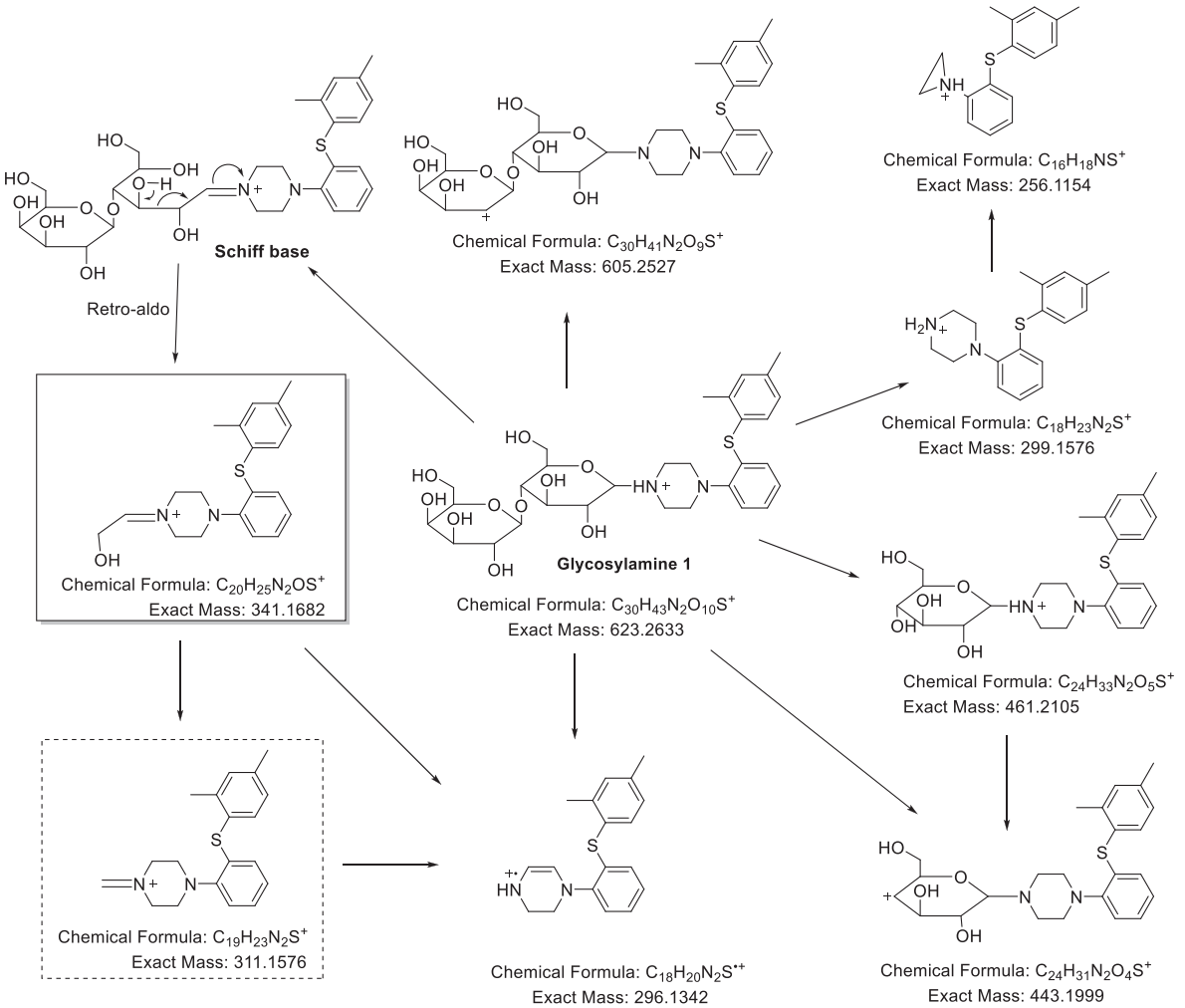

SCHEME 2 Proposed fragmentation pathways of the precursor protonated glycosylamine 1 (*m/z* 623)

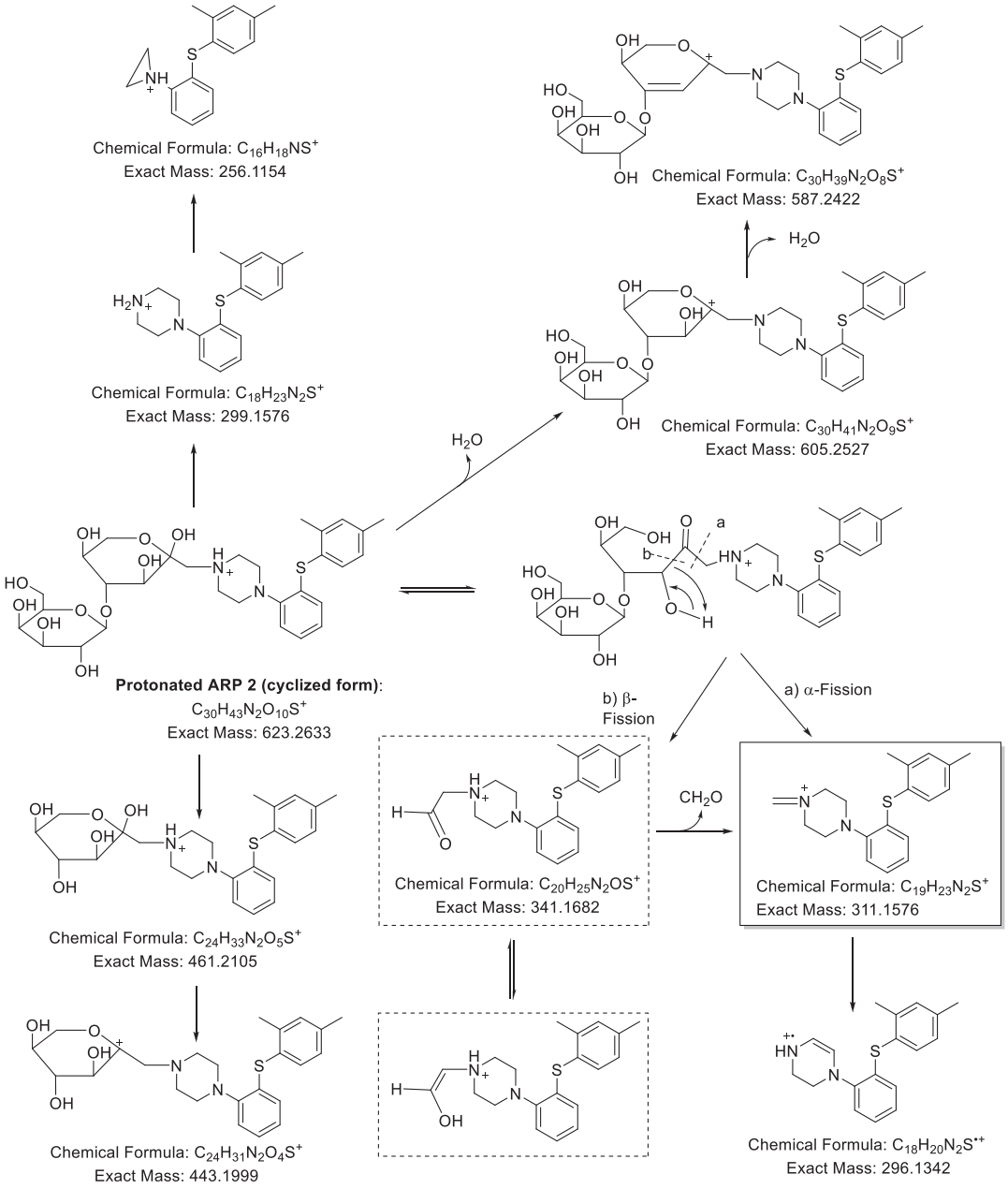

SCHEME 3 Proposed fragmentation pathways of the precursor protonated ARP 2 (*m/z* 623)

3.6.2 | Characteristic ions in glycosylamine 1 and ARP 2

After carefully comparing the MS^2 spectra, we found that the product ions of the obtained glycosylamine 1 and ARP 2 were very similar, except for some differences in abundance. As shown in Figure 3, most of the product ions of glycosylamine 1 are the same as those of ARP 2. The common product ions observed are *m/z* 605 (loss of H_2O), 587 (loss of two H_2O), 461 (loss of $C_6H_{11}O_5$), 443 (loss of H_2O and $C_6H_{11}O_5$), and two smaller fragments (*m/z* 299 and 256) containing the core structure of vortioxetine. Nevertheless, two characteristic phenomena between the two MS^2 spectra can be observed: (1) the abundance of *m/z* 341 is much greater than the abundance of *m/z* 311 in glycosylamine 1 and the ratio of *m/z* 341 to *m/z* 311 is ~32. (2) The abundance of *m/z* 311 is greater than the abundance of *m/z* 341 in ARP 2 and the ratio of *m/z* 311 to *m/z* 341 is ~11. Based on the above fragments observed and structures of the two isomers, the probable structures of *m/z* 341 (Figure 4A) and 311 (Figure 4B) can be proposed. For the predominant formation of the *m/z* 341 fragment from the Schiff base (the open-ring form of glycosylamine 1), it apparently can be attributed to the facile cleavage of the C-2–C-3 bond (of the glucose moiety) via a retro-aldo mechanism of the Schiff base; this cleavage is analogous to

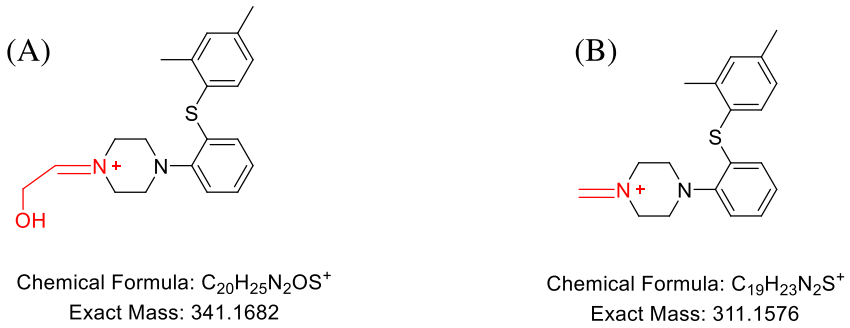

FIGURE 4 Characteristic structures of the prominent product ions from protonated glycosylamine 1 (*m/z* 341) and protonated ARP 2 (*m/z* 311) generated from vortioxetine and lactose

the one in the Schiff base formed between glycine and glucose as described by Xing et al.[21] On the other hand, the preferential formation of the *m/z* 311 fragment (versus that of the *m/z* 341 fragment) from ARP 2 can be attributed to the α-fission of the C-1–C-2 bond of the glucose moiety.[21,24–25]

Based on the MS^2 fingerprints of the two degradants (1, 2) obtained, two characteristic MS^2 fragments were observed: one is $[M_{vort} + C_2H_3O]^+$ at *m/z* 341 (M_{vort} is the vortioxetine core), while the other is $[M_{vort} + CH]^+$ at *m/z* 311. The fragment of $[M_{vort} + C_2H_3O]^+$ at *m/z* 341, which will be referred to as the C2 fragment, is much more prominent from protonated glycosylamine 1, while the fragment of $[M_{vort} + CH]^+$ at *m/z* 311, which will be referred to as the C1 fragment, is much more prominent from protonated ARP 2.

3.7 | Results from using different CEs and different MS instruments

The above results were obtained using a collision energy of 30 eV on the Agilent LC/QTOF mass spectrometer, and, at this CE, abundant fragments can often be obtained. In fact, we have also examined CEs other than 30 eV during the MS^2 experiments, such as 20 eV and 40 eV. At 20 eV, the ratio of C2 to C1 in glycosylamine 1 is 47, while the ratio of C1 to C2 in ARP 2 is 12. At a CE of 40 eV, the ratio of C2 to C1 in glycosylamine 1 is 12 and the ratio of C1 to C2 in ARP 2 is 13.

The results are summarized in Table 3, along with other model systems (the results of the latter will be discussed in section 3.8). It can be clearly seen that the ratio of C2/C1 in the glycosylamines decreases as the CE increases for all the model systems examined. On the other hand, no such clear trend can be observed for the ratio of C1/C2 in the ARPs examined.

In addition, we also performed a sub-set of the vortioxetine experiments (with three reducing sugars) on the Shimadzu LC/IT-TOF mass spectrometer, an MS instrument with very different configuration. The results show that the same rule prevails: i.e., the C2 fragment is significantly higher than C1 in the glycosylamines, while the C1 fragment is significantly higher than C2 in the ARPs (Table 4).

The above phenomena indicate that glycosylamines and ARPs can respectively produce C1 and C2 fragments with consistent

TABLE 3 The C2/C1 ratio in MS^2 of protonated glycosylamines (1, 3, 5, 7, 9, 11) and C1/C2 ratio in MS^2 of protonated ARPs (2, 4, 6, 8, 10, 12) at different collision energies

		C2/C1 (glycosylamine)			C1/C2 (ARP)		
Amine compound	**Reducing sugar**	**20 eV**	**30 eV**	**40 eV**	**20 eV**	**30 eV**	**40 eV**
Vortioxetine	Glucose	42 (3)	11 (3)	5.3 (3)	6.0 (4)	8.5 (4)	11 (4)
Vortioxetine	Galactose	41 (5)	12 (5)	4.2 (5)	11 (6)	10 (6)	15 (6)
Vortioxetine	Lactose	47 (1)	32 (1)	12 (1)	12 (2)	11 (2)	13 (2)
α-Phenylethylamine	Lactose	29 (7)	13 (7)	6.5 (7)	20 (8)	11 (8)	5.2 (8)
1-Phenylpiperazine	Lactose	61 (9)	12 (9)	7.0 (9)	1.4 (10)	2.0 (10)	4.5 (10)
Benzylamine	Lactose	6.0 (11)	3.1 (11)	1.8 (11)	15 (12)	8.5 (12)	8.0 (12)

All data were obtained on the Agilent LC/QTOF instrument (refer to section 2.3).

TABLE 4 The C2/C1 ratio in MS^2 of protonated glycosylamines (1, 3, 5) and C1/C2 ratio in MS^2 of protonated ARPs (2, 4, 6) on different MS instruments

		C2/C1 (glycosylamine)		C1/C2 (ARP)	
Amine compound	**Reducing sugar**	**QTOF-MS**	**IT-TOF-MS**	**QTOF-MS**	**IT-TOF-MS**
Vortioxetine	Lactose	32 (1)	16 (1)	11 (2)	20 (2)
Vortioxetine	Glucose	11 (3)	21 (3)	8.5 (4)	5.0 (4)
Vortioxetine	Galactose	12 (5)	19 (5)	10 (6)	10 (6)

For the analytical methods, refer to section 2.3.

TABLE 5 C2/C1 and C1/C2 ratios of fragments in glycosylamines (all compounds with odd numbers) and ARPs (all compounds with even numbers) of the eight model systems

Model	Amine compound	Reducing sugar	C1 fragment	C2 fragment	C2/C1 (glycosyl amine)	C1/C2 (ARP)
Primary amine + disaccharide	α-Phenylethylamine	Lactose	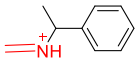 Chemical Formula: $C_9H_{12}N^+$ Exact Mass: 134.0964	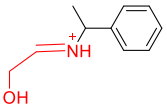 Chemical Formula: $C_{10}H_{14}NO^+$ Exact Mass: 164.1070	13 (7)	11 (8)
	Benzylamine	Lactose	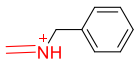 Chemical Formula: $C_8H_{10}N^+$ Exact Mass: 120.0808	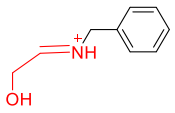 Chemical Formula: $C_9H_{12}NO^+$ Exact Mass: 150.0913	3.1 (11)	8.5 (12)
Primary amine + monosaccharide	Benzylamine	Glucose	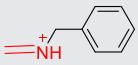 Chemical Formula: $C_8H_{10}N^+$ Exact Mass: 120.0808	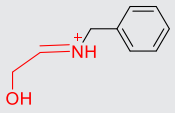 Chemical Formula: $C_9H_{12}NO^+$ Exact Mass: 150.0913	3.0 (13)	5.0 (14)
	Benzylamine	Galactose	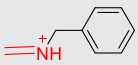 Chemical Formula: $C_8H_{10}N^+$ Exact Mass: 120.0808	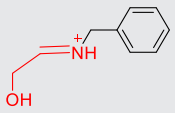 Chemical Formula: $C_9H_{12}NO^+$ Exact Mass: 150.0913	2.1 (15)	5.0 (16)
Secondary amine + disaccharide	Vortioxetine	Lactose	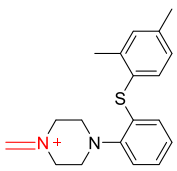 Chemical Formula: $C_{19}H_{23}N_2S^+$ Exact Mass: 311.1576	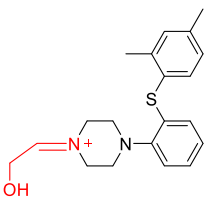 Chemical Formula: $C_{20}H_{25}N_2OS^+$ Exact Mass: 341.1682	32 (1)	11 (2)
	1-Phenylpiperazine	Lactose	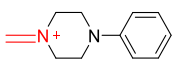 Chemical Formula: $C_{11}H_{15}N_2^+$ Exact Mass: 175.1230	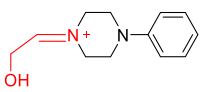 Chemical Formula: $C_{12}H_{17}N_2O^+$ Exact Mass: 205.1335	12 (9)	2.0 (10)

TABLE 5 (Continued)

Model	Amine compound	Reducing sugar	C1 fragment	C2 fragment	C2/C1 (glycosyl amine)	C1/C2 (ARP)
Secondary amine + monosaccharide	Vortioxetine	Glucose	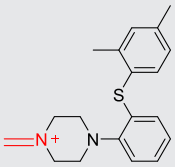 Chemical Formula: $C_{19}H_{23}N_2S^+$ Exact Mass: 311.1576	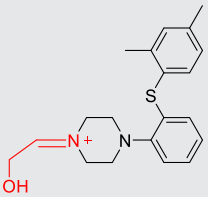 Chemical Formula: $C_{20}H_{25}N_2OS^+$ Exact Mass: 341.1682	11 (3)	8.5 (4)
	Vortioxetine	Galactose	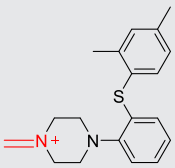 Chemical Formula: $C_{19}H_{23}N_2S^+$ Exact Mass: 311.1576	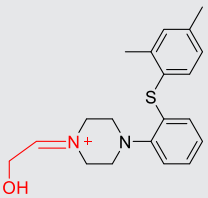 Chemical Formula: $C_{20}H_{25}N_2OS^+$ Exact Mass: 341.1682	12 (5)	10 (6)

All data were obtained on the Agilent LC/QTOF mass spectrometer (refer to section 2.3). The data for benzylamine with glucose or galactose were obtained at a CE of 20 eV, and the data for other model systems were obtained at a CE of 30 eV.

preference for one fragment over the other, under different CEs and on different instruments. Therefore, it can be envisioned that the preference for either the C1 or C2 fragment, i.e., the ratio of C1/C2 or C2/C1, can be utilized to distinguish glycosylamines from ARPs.

3.8 | Analysis of the C1 and C2 fragments in glycosylamines and ARPs from other model systems

In order to verify whether the preference for either the C1 or C2 fragment is limited to vortioxetine or may be universally applicable to other primary and secondary amines, we replaced vortioxetine with α-phenylethylamine, 1-phenylpiperazine, and benzylamine, respectively, in the Maillard reaction with lactose. Likewise, we also replaced lactose with glucose and galactose, respectively, in the Maillard reaction with vortioxetine (refer to section 2.9). The MS^2 results are shown in Figures S5–S11 (supporting information) and the C2/C1 ratios in the glycosylamines and C1/C2 ratios in the ARPs are summarized in Table 5. Again, the same rule prevails: the abundance of the C2 fragment is much greater than the abundance of C1 in the glycosylamines and the ratio of C2/C1 ranged from 2.1 to 32 in the seven model systems. On the other hand, the abundance of the C1 fragment is greater than the abundance of C2 in ARPs and the ratio of C1/C2 ranged from 2.0 to 11 in the ARPs produced by the seven model systems.

4 | CONCLUSIONS

In this study, we prepared and fully characterized the glycosylamine and Amadori rearrangement products formed between vortioxetine and lactose, two impurities that have not been reported previously. The MS^2 fingerprints of the two degradants display significantly different profiles, despite the fact that many common fragments are observed. Specifically, the protonated glycosylamine shows a prominent characteristic fragment of $[M_{vort} + C_2H_4O]^+$ at *m/z* 341 (C2 fragment), while the protonated ARP shows a prominent characteristic fragment of $[M_{vort} + CH]^+$ at *m/z* 311 (C1 fragment). Further study of the Maillard reactions between several other structurally diverse primary/secondary amines and lactose, as well as other reducing sugars, produced similar patterns.

The study suggests that the characteristic C1 and C2 fragments and their ratios may be used to differentiate the glycosylamine and ARP degradants, the two isomeric degradants of the Maillard reaction, which are commonly encountered in finished dosage forms of pharmaceutical products containing primary and secondary amine APIs. Our results are consistent with those that have just been

published by Xing et al,[21,22] in which they reported that MS/MS fragmentation patterns can be used to discriminate between glucose-derived Schiff bases, Amadori, and Heyns compounds with several amino acids. Their work as well as ours indicates that this methodology can be generally applicable for differentiating the early-stage isomeric Maillard products from amino compounds of vastly different structures with reducing sugars.

PEER REVIEW

The peer review history for this article is available at https://publons.com/publon/10.1002/rcm.9062.

ORCID

Min Li https://orcid.org/0000-0001-8690-3451

REFERENCES

1. Gandhi S, Ren D, Xiao G, et al. Elucidation of degradants in acidic peak of cation exchange chromatography in an IgG1 monoclonal antibody formed on long-term storage in a liquid formulation. *Pharm Res*. 2012;29(1):209-224.
2. Bhattacharya A, Cui Y. A GPU-accelerated algorithm for biclustering analysis and detection of condition-dependent coexpression network modules. *Sci Rep*. 2017;7(1):4162.
3. Abdoh A, Al-Omari MM, Badwan AA, Jaber AM. Amlodipine besylate–excipients interaction in solid dosage form. *Pharm Dev Technol*. 2004;9(1):15-24.
4. Murakami T, Fukutsu N, Kondo J, Kawasaki T, Kusu F. Application of liquid chromatography-two-dimensional nuclear magnetic resonance spectroscopy using pre-concentration column trapping and liquid chromatography–mass spectrometry for the identification of degradant products in stressed commercial amlodipine maleate tablets. *J Chromatogr A*. 2008;1181(1–2):67-76.
5. Serajuddin ATM, Thakur AB, Ghoshal RN, et al. Selection of solid dosage form composition through drug–excipient compatibility testing. *J Pharm Sci*. 1999;88(7):696-704.
6. Hodge JE. Dehydrated foods – chemistry of browning reactions in model systems. *J Agric Food Chem*. 1953;1(15):625-651.
7. Arena S, Renzone G, D'Ambrosio C, Salzano AM, Scaloni A. Dairy products and the Maillard reaction: A promising future for extensive food characterization by integrated proteomics studies. *Food Chem*. 2017;219:477-489.
8. Li M. Organic chemistry of drug degradation. In: *Drug–Excipient Interactions and Adduct Formation*. Cambridge: Royal Society of Chemistry; 2012.
9. Li M, Conrad B, Maus RG, et al. A novel oxidative degradation pathway of indomethacin under the stressing by hydrogen peroxide. *Tetrahedron Lett*. 2005;46(20):3533-3536.
10. Li M, Wang X, Chen B, Chan TM, Rustum A. Forced degradation of betamethasone sodium phosphate under solid state: Formation, characterization, and mechanistic study of all four 17,20-diastereomers of betamethasone 17-deoxy-20-hydroxy-21-oic acid. *J Pharm Sci*. 2009;98(3):894-904.
11. Wang X, Peng Y, Li M, Rustum AM. Use of high resolution LC–MS^n analysis in conjunction with mechanism-based stress studies: Identification of asarinin, an impurity from sesame oil in an animal health product. *J Pharm Biomed Anal*. 2009;50(5):1015-1021.
12. Li M, Chen B, Monteiro S, Rustum AM. Mechanism of base-catalyzed autooxidation of corticosteroids containing 20-keto-21-hydroxyl side chain. *Tetrahedron Lett*. 2009;50(32):4575-4581.
13. Jin J, Wang Z, Lin J, Zhu W, Gu C, Li M. "Ghost peaks" of ezetimibe: Solution degradant products of ezetimibe in acetonitrile induced by alkaline impurities from glass HPLC vials. *J Pharm Biomed Anal*. 2017;140:281-286.
14. Lin J, Lin Z, Li D, et al. "Ghost peak" of clofazimine: A solution degradant product of clofazimine via nucleophilic substitution by nitrite leaching from certain glass HPLC vials. *J Pharm Biomed Anal*. 2018;150:183-190.
15. Lin J, Huang T, Feng M, et al. Solution degradant of mirabegron extended release tablets resulting from a Strecker-like reaction between mirabegron, minute amounts of hydrogen cyanide in acetonitrile, and formaldehyde in PEG during sample preparation. *J Pharm Biomed Anal*. 2019;168:181-188.
16. Lin J, Liu X, Wang J, et al. An artifactual solution degradant of pregabalin due to adduct formation with acetonitrile catalyzed by alkaline impurities during HPLC sample preparation. *J Pharm Biomed Anal*. 2019;175:112788.
17. Tian Y, Lin J, Chen F, et al. Structure elucidation and formation mechanistic study of a methylene-bridged pregabalin dimeric degradant in pregabalin extended-release tablets. *Int J Pharm*. 2019;575:118910.
18. Li M, Wang X, Chen B, et al. Use of liquid chromatography/tandem mass spectrometric molecular fingerprinting for the rapid structural identification of pharmaceutical impurities. *Rapid Commun Mass Spectrom*. 2010;23(22):3533-3542.
19. Connolly KR, Thase ME. Vortioxetine: A new treatment for major depressive disorder. *Expert Opin Pharmacother*. 2016;17(3):421-431.
20. Lovdahl MJ, Hurley TR, Tobias B, Priebe SR. Synthesis and characterization of pregabalin lactose conjugate degradant products. *J Pharm Biomed Anal*. 2002;28(5):917-924.
21. Xing H, Mossine VV, Yaylayan V. Diagnostic MS/MS fragmentation patterns for the discrimination between Schiff bases and their Amadori or Heyns rearrangement products. *Carbohydr Res*. 2020;491:107985.
22. Xing H, Yaylayan V. Mechanochemical generation of Schiff bases and Amadori products and utilization of diagnostic MS/MS fragmentation patterns in negative ionization mode for their analysis. *Carbohydr Res*. 2020;491:108091.
23. Lin J, Huang T, Lan F, et al. N-Formyl vortioxetine and preparation method therefore and solid preparation of vortioxetine: CN, WO 2019/056211 A1. 2019-03-28.
24. Hoaglund HCS, Williamson ML, Jansen PJ, et al. Mechanistic studies of the N-formylation of edivoxetine, a secondary amine-containing drug, in a solid oral dosage form. *J Pharm Sci*. 2017;106(5):1218-1238.

SUPPORTING INFORMATION

Additional supporting information may be found online in the Supporting Information section at the end of this article.

How to cite this article: Wang S, Lin J, Li D, et al. Study of the isomeric Maillard degradants, glycosylamine and Amadori rearrangement products, and their differentiation via MS^2 fingerprinting from collision-induced decomposition of protonated ions. *Rapid Commun Mass Spectrom*. 2021;35:e9062. https://doi.org/10.1002/rcm.9062